# Mild Hydrothermal-Reduction Synthesis and Mössbauer Study of Low-Dimensional Iron Chalcogenide Microcrystals and Single Crystals

Yi Xie,* Liying Zhu, Xuchuan Jiang, Jun Lu, Xiuwen Zheng, Wei He, and Yuzhi Li

*Structure Research Lab and Lab of Nanochemistry & Nanomaterials, University of Science & Technology of China, Hefei, Anhui 230026, People's Republic of China*

Low-dimensional iron chalcogenide $Fe_7S_8$ and $FeSe_2$ microcrystals and $FeTe_2$ bulk single crystals were synthesized via the reactions of $FeCl_3$ with S or Se or Te powders in hydrazine hydrate solution (85%, v/v) at 140 °C for 36 h. The products were characterized by means of X-ray powder diffraction, rocking curve, transmission electron microscopy, electron diffraction, and scanning electron microscopy techniques. In the reaction process, hydrazine hydrate can coreduce $Fe^{3+}$ and elemental chalcogen to $Fe^{2+}$ and chalcogen anions, respectively, the combination of which can lead to the reaction proceeding completely. The morphologies of the products are affected by the temperature, pressure, and pH values. Moreover, a suitable speed of decreasing the temperature and proper supersaturation are two important factors in the formation of single-crystal $FeTe_2$. Mössbauer spectra show the magnetism of $Fe_7S_8$ and nonmagnetic properties for $FeSe_2$ and $FeTe_2$ at room temperature.

## Introduction

Low-dimensional crystal structures, such as wirelike, needlelike, and platelike structures, and thin films are currently the focus of much attention due to their special properties.[1] These fascinating systems are expected to exhibit remarkable mechanical properties, and electrical, optical, and magnetic properties which are quite different from those of their corresponding polycrystal powder materials. Such low-dimensional crystalline materials have potential applications in molecular-based electronic devices, such as in optical memory and switches, display, and data records.

Many studies have been done on iron dichalcogenides with two fundamental modifications of pyrite and marcasite, containing the narrow 3d band (about 1.0 eV), which are known to exhibit good magnetic properties,[2] as well as semiconductivity,[3] such as high electrical conductivity,[4–6] high thermoelectric powder values,[4,6] and the Hall coefficient.[5,7] The pyrrhotite $Fe_7S_8$, with monoclinic, trigonal, and hexagonal structures, has been extensively studied due to its interesting ferromagnetic properties[8] and complex crystalline structure.[9]

Traditionally, metal chalcogenides are synthesized by the elemental reaction in evacuated tubes at elevated temperature,[10–12] or by reaction of aqueous metal salt solutions with toxic and malodorous gas $H_2E$[13] (E = S, Se, or Te). Iron chalcogenides are also obtained by the method of rapidly quenched ternary.[14,15] However, there are few reports on the preparation of bulk single crystals $FeTe_2$ and microcrystals $Fe_7S_8$ and $FeSe_2$. Conventionally, the iron chalcogenide bulk single crystals have mainly been grown by vapor-phase methods, such as the chemical vapor transport technique using $AlBr_3$ and $I_2$ as transporting agents[16] and the closed-tube vapor transport technique.[17] The above-mentioned methods generally require special, complicated devices, or sophisticated techniques. Moreover, the growth temperature is higher (>600 °C), and the temperature gradient has to be carefully controlled.

Recently, the hydrothermal-reduction route (HRR) has been developed as a mild and effective route to synthesize novel materials. Several kinds of nanocrys-

* To whom correspondence should be addressed. E-mail: yxie@ustc.edu.cn.

(1) Rao, A. M.; Richter, E.; Bandow, S.; Chase, B.; Eklund, P. C.; Williams, K. A.; Fang, S.; Subbaswamy, K. R.; Menon, M.; Thess, A.; Smalley, R. E.; Dresselhaus, G.; Dresselhaus, M. S. *Science* **1997**, *275*, 187.

(2) Zhang, J. H.; Wu B.; O'Connor C. J.; Simmons, W. B. *J. Appl. Phys.* **1993**, *10*, 73.

(3) Dudkin L. D.; Vaidanich V. I. *Sov. Phys. Solid State* **1961**, *2*, 138.

(4) Bither, T. A.; Bouchard, R. J.; Cloud, W. H.; Donohue, P. C.; Siemens, W. J. *Inorg. Chem.* **1968**, *7*, 2208.

(5) Fisher, G. *Can. J. Phys.* **1958**, *36*, 1435.

(6) Dudkin, L. D.; Vaidanich, V. I. *Sov. Phys. Solid State* **1962**, *6*, 1384.

(7) Hulliger, F. *Helv. Phys. Acta* **1962**, *35*, 535.

(8) Besnus M. J.; Meyer, A. P. *J. Proc. Int. Conf. Magn., Nottingham* **1964**, 507. Sato, K. *J. Phys. Soc. Jpn.* **1966**, *21*, 733.

(9) Li, F.; Franzen, H. F. *J. Solid State Chem.* **1996**, *126*, 108. Nakano, A.; Tokonami, M.; Morimoto, N. *Acta Crystallogr.* **1979**, *B35*, 722.

(10) Harada, T. *J. Phys. Soc. Jpn.* **1998**, *67* (4), 1352.

(11) Kjekshus, A.; Rakke, T.; Andresen, A. F. *Acta Chem. Scand., A* **1974**, *28*, 996.

(12) O'Reilly, W.; Hoffmann, V.; Chouker, A. C.; Soffel, H. C.; Menyeh, A. *Geophys. J. Int.* **2000**, *142*, 669.

(13) Dusastre, V.; Omar, B.; Parkin, I. P.; Shaw, G. A. *J. Chem. Soc., Dalton Trans.* **1997**, 3505.

(14) Foutana, M.; Bormioli, M.; Arondo, B. *J. Non-Cryst. Solids* **1998**, *231*, 234.

(15) Haushalter, R. C.; O'Connor, C. J.; Umarji, A. M.; Shenoy, G. K.; Saw, C. K. *Solid State Commun.* **1984**, *49* (10), 929.

(16) Pickardt, J.; Reuter, B.; Riedel, E.; Söchtig, J. *J. Solid State Chem.* **1975**, *15*, 366.

(17) Bouchard, R. J. *J. Cryst. Growth* **1968**, *2*, 40.

talline chalcogenides have been synthesized through such a process.[18] Here, we extend the HRR method to prepare low-dimensional iron chalcogenide crystals. The flakelike crystals $Fe_7S_8$, rodlike crystals $FeSe_2$, and rodlike single crystals $FeTe_2$ were successfully prepared via the mild HRR method at lower temperature in hydrazine hydrate solution (85%, v/v), which is not only alkaline but also a strong reductant. On the other hand, its oxidation product is the clean $N_2$, so harmful impurities will not been introduced into the system. Inorganic materials with different morphologies which have the same chemical composition may exhibit different physical properties.[19] The thin platelets prepared by our HRR method provide desirable crystals to be used for physical property measurements. Moreover, the hydrothermal method is a suitable method to study the growth mechanism of single crystals.

## Experimental Section

Analytical grade solvents and reagents were purchased from Shanghai Chemistry Co. Ltd. $FeTe_2$ was prepared as follows: A 0.325 g (2 mmol) sample of anhydrous $FeCl_3$ and a 0.254 g (2 mmol) sample of Te powders were added to a Teflon-lined autoclave of 50 mL capacity with hydrazine hydrate solution (85%, v/v) up to 75% of the total volume. The autoclave was heated and maintained at 140 °C for 36 h, and then gradually cooled to room temperature. All of the rodlike crystals, metallic light gray in color with a high reflective luster, were carefully collected, washed with distilled water and ethanol several times, respectively, and dried in a vacuum at 60 °C for 4 h. The yield of rodlike crystals was about 85% through weight analysis of the prepared products, with the existence of small amounts of solid powders. Both rodlike single crystals and solid powders are pure phases of $FeTe_2$ according to the X-ray powder diffraction (XRD) analysis. In the case of the preparation of other chalcogenides, the processes were similar to that of $FeTe_2$, just using S or Se powders with a molar ratio of 1:1 of $FeCl_3$ to S or Se, and the final black precipitates were collected for characterization.

The phase and the crystallographic structure of the products were determined by XRD using a Japan Rigaku D/max-rA X-ray diffractometer with Cu Kα radiation ($\lambda = 1.54178$ Å). A scan rate of 0.05 deg/s was applied to record the patterns in the $2\theta$ range of 10–70°. And further judgment of the single crystal was confirmed by the rocking curve. The morphology and size of the products were observed by transmission electron microscopy (TEM), taken on a Hitachi model H-800 under an accelerating voltage of 200 kV, and scanning electronic microscopy (SEM), performed on an X-650 scanning electron microanalyzer. To study the structure of the products, electronic diffraction (ED) patterns taken on a Hitachi model H-800 were used. The magnetic behavior of the products was studied by Mössbauer spectroscopy, via an Oxford MS-500 spectrometer with a 25 mCi $Co^{57}$ source in Pd on a constant acceleration drive at room temperature.

## Results and Discussion

It is well-known that the intermediate pyrrhotite $Fe_{1-x}S$ has a complex structure, which often has a superstructure of the NiAs type with various incommensurate periods. Especially, $Fe_7S_8$ has three kinds of typical structures, monoclinic, trigonal, and hexagonal, due to the difference in vacancies. The monoclinic and trigonal $Fe_7S_8$ have ordered vacancies, and thus
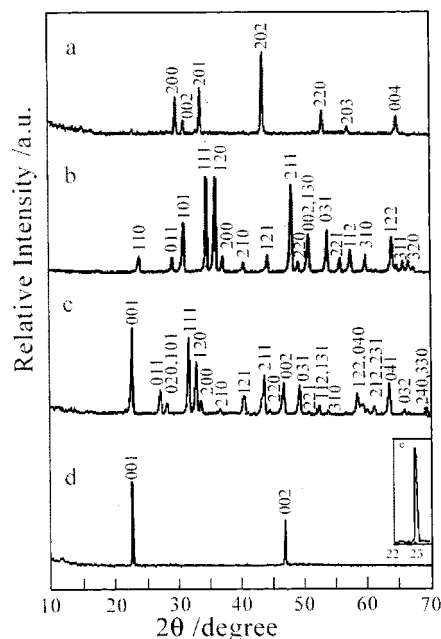
(18) Yang, J.; Yu, S. H.; Han, Z. H.; Qian, Y. T.; Zhang, Y. H. *J. Solid State Chem.* **1999**, *146*, 387. Zhan, J. H.; Xie, Y.; Yang, X. G.; Zhang, W. X.; Qian, Y. T. *J. Solid State Chem.* **1999**, *146*, 36. Wang, C.; Li, Y. D.; Zhang, G. H.; Shen, G. Q. *Inorg. Chem.* **2000**, *39*, 4237.
(19) Hulliger, J. *Angew. Chem., Int. Ed. Engl.* **1994**, *33*, 143.



**Figure 1.** (a) XRD patterns of the microcrystals $Fe_7S_8$. (b) XRD patterns of the microcrystals $FeSe_2$. (c) XRD patterns of polycrystal $FeTe_2$ powders from single crystals. (d) XRD patterns of single crystals $FeTe_2$. (e) Rocking curve of single crystals $FeTe_2$.

have a lattice of lower symmetry, while hexagonal $Fe_7S_8$ has a lattice of higher symmetry because of a disordered vacancy. In marcasite $FeE_2$ (E = Se, Te) with space group $P_{nnm}$ (58), an iron atom in the crystal lattices, surrounded octahedrally by six chalcogen atoms, forms hybrid $d^2sp^3$ bonds, and two neighboring coordination octahedra share an edge, while one chalcogen E (E = S, Se, or Te) atom has a tetrahedral neighborhood, and is bonded to three iron atoms and one E atom.

The XRD patterns of the products prepared in our mild hydrothermal process are shown in Figure 1. In each of the XRD patterns, all the reflections can be indexed to those of the corresponding pure phases and are consistent with those of standard samples. The phases and lattice parameters of the samples are listed in Table 1. The XRD pattern (Figure 1c) of the powders ground from a single crystal is a little different from that of the common polycrystallite $FeTe_2$ powders, and the strongest peak of the former is the (001) plane rather than the (111) plane in common polycrystalline $FeTe_2$ powders. And the XRD pattern of rodlike single-crystal $FeTe_2$ (Figure 1d) only exhibits two peaks at $2\theta$ = 23.3° and 46.6°, which can be assigned to the orthorhombic (001) plane and (002) plane, respectively. Meanwhile, the other relatively strong reflection peaks such as the (111) and (112) planes in polycrystallite powder diffraction ground from a single crystal are absent in this pattern. The above results show that the (001) plane of the $FeTe_2$ crystals parallels the shaft of the rodlike single crystals. And the rocking curve of the (001) reflection for $FeTe_2$ single crystals (Figure 1e) indicates that the products have perfect orientation of the single crystal.

TEM images and ED patterns for the products are shown in Figure 2. The $Fe_7S_8$ crystals (Figure 2a) display a regular hexagonal thin platelike shape with dimensions of ca. 1 $\mu$m × 1 $\mu$m, and from their ED
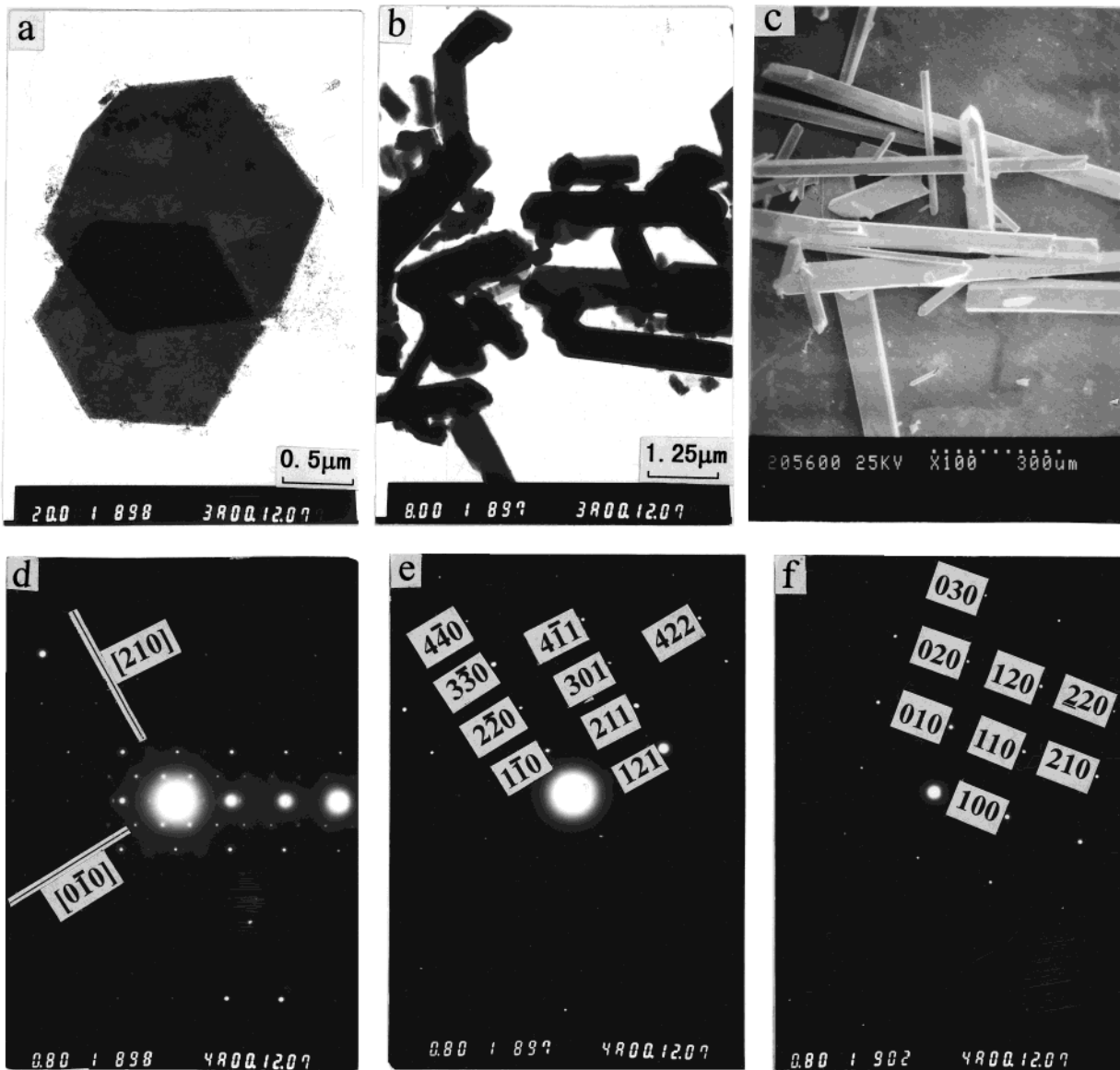
**Figure 2.** TEM images of the products (a) $Fe_7S_8$ and (b) $FeSe_2$. SEM image of the products (c) single crystals $FeTe_2$. ED patterns of the products (d) $Fe_7S_8$, (e) $FeSe_2$, and (f) $FeTe_2$.

**Table 1. Characterization of the Products**

| product | phase | lattice parameters (Å) | | morphology | TEM size |
| | | exptl | lit.[20] | | |
| --- | --- | --- | --- | --- | --- |
| $Fe_7S_8$ | hexagonal | $a = 6.90$ | $a = 6.93$ | hexagonal | $1\ \mu m \times 1\ \mu m$ |
| | | $c = 5.76$ | $b = 5.75$ | platelike | |
| $FeSe_2$ | orthorhombic | $a = 4.81$ | $a = 4.81$ | rodlike | $(1-10\ \mu m) \times (0.5-1\ \mu m)$ |
| | | $b = 5.81$ | $b = 5.80$ | | |
| | | $c = 3.60$ | $c = 3.58$ | | |
| $FeTe_2$ | orthorhombic | $a = 5.29$ | $a = 5.30$ | rodlike | $(0.2-0.6\ cm) \times (20-70\ \mu m)$ |
| | | $b = 6.27$ | $b = 6.27$ | | |
| | | $c = 3.86$ | $c = 3.91$ | | |

pattern (Figure 2d), a reciprocal lattice plane is identified perpendicular to the *c* axis when an electron beam is perpendicular to the flake. Extra reflections occur at the midpoints between the usual spots for a NiAs-type sublattice, showing the existence of a superlattice with $a = 2A$, where *a* and *A* are the lattice para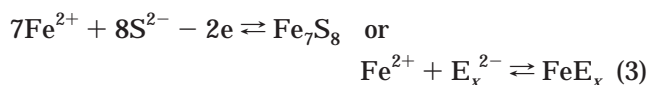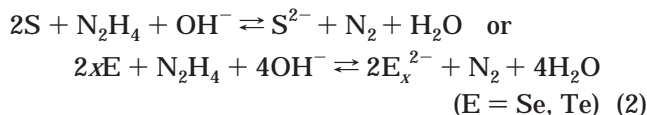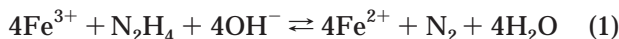meters of the superlattice and the sublattice, respectively.[21] Fig-ure 2b for the $FeSe_2$ crystals exhibits rodlike morphology with lengths of ca. $1-10\ \mu m$ and diameters of ca. $0.5-1$ $\mu m$. The ED pattern (Figure 2e) indicates that the $FeSe_2$ crystals grow along the $[1\bar{1}3]$ axis. According to the SEM images (Figure 2c), the single crystals $FeTe_2$ are rodlike crystals with sizes of ca. $0.2-0.6\ cm \times 20-70\ \mu m$, and the typical ED pattern for the crystal (Figure 2f) shows that rodlike single crystals grow along the *c* axis.

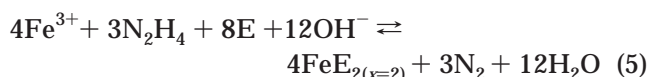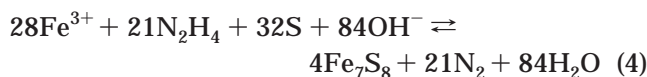In this hydrothermal-reduction process, hydrate hy-drazine plays an important role in the formation of pure-

(20) JCPDS card file: $Fe_7S_8$, no. 25-411; $FeSe_2$, no. 12-291; $FeTe_2$, no. 14-419.

(21) Horiuchi, S.; Wada, H. *Acta Crystallogr.* **1971**, *B27*, 504.

phase $Fe_7S_8$ and $FeSe_2$ microcrystals and $FeTe_2$ bulk single crystals. The reaction mechanism may be based on a coreduction pathway under the alkaline medium, namely, the fact that hydrazine hydrate can coreduce $Fe^{3+}$ and elemental chalcogen to $Fe^{2+}$ and chalcogen anions simultaneously, the combination of which produces the desired chalcogenides. The proposed reaction mechanism can be described as
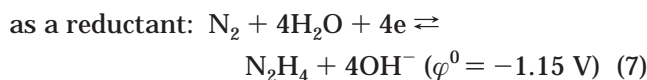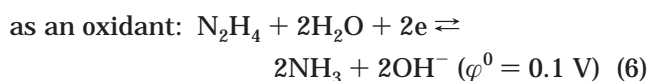
$$4Fe^{3+} + N_2H_4 + 4OH^- \rightleftharpoons 4Fe^{2+} + N_2 + 4H_2O \quad (1)$$

$$2S + N_2H_4 + OH^- \rightleftharpoons S^{2-} + N_2 + H_2O \quad \text{or}$$
$$2xE + N_2H_4 + 4OH^- \rightleftharpoons 2E_x^{2-} + N_2 + 4H_2O$$
$$(E = Se, Te) \quad (2)$$

$$7Fe^{2+} + 8S^{2-} - 2e \rightleftharpoons Fe_7S_8 \quad \text{or}$$
$$Fe^{2+} + E_x^{2-} \rightleftharpoons FeE_x \quad (3)$$

and the total process is expressed by the following equations:

$$28Fe^{3+} + 21N_2H_4 + 32S + 84OH^- \rightleftharpoons$$
$$4Fe_7S_8 + 21N_2 + 84H_2O \quad (4)$$

$$4Fe^{3+} + 3N_2H_4 + 8E + 12OH^- \rightleftharpoons$$
$$4FeE_{2(x=2)} + 3N_2 + 12H_2O \quad (5)$$

The oxidition ability of elemental Se and Te ($\varphi^0_{Se/Se2-} = -0.92$ V, $\varphi^0_{Te/Te2-} = -1.14$ V) is weaker than that of elemental S ($\varphi^0_{S/S2-} = -0.48$ V), so hydrazine hydrate cannot reduce them to the lowest valence $E^{2-}$ but can to the lower valence $E_x^{2-}$. The intermediate pyrrhotite $Fe_7S_8$ is inclined to form due to the existence of the random distribution of the vacancy.[9]

To further understand the proposed mechanism of the formation of chalcogenides, we can prove it from Latimer potentials

as an oxidant:  $N_2H_4 + 2H_2O + 2e \rightleftharpoons$
$$2NH_3 + 2OH^- \; (\varphi^0 = 0.1 \text{ V}) \quad (6)$$

as a reductant:  $N_2 + 4H_2O + 4e \rightleftharpoons$
$$N_2H_4 + 4OH^- \; (\varphi^0 = -1.15 \text{ V}) \quad (7)$$

The Latimer potentials of iron under an alkaline medium are given above the arrows:

$$Fe(OH)_3 \xrightarrow{-0.56 \text{ V}} Fe(OH)_2 \xrightarrow{-0.887 \text{ V}} Fe \quad (8)$$

The cell potential at which hydrazine hydrate oxidizes $Fe(OH)_2$ to $Fe(OH)_3$ is 0.66 V, and that at which $N_2H_4$ reduces $Fe(OH)_2$ to Fe is 0.273 V. By means of the above calculation of the cell potential, it can be concluded that $N_2H_4$ is apt to oxidize $Fe^{2+}$, and $Fe^{2+}$ cannot be reduced to Fe in the alkaline medium.[22] Hence, $Fe^{3+}$ can be reduced to $Fe^{2+}$, and the reaction process is not that of element combination but that of ion combination. The quantity of reaction heats given off can drive the reaction to occur at lower temperature.
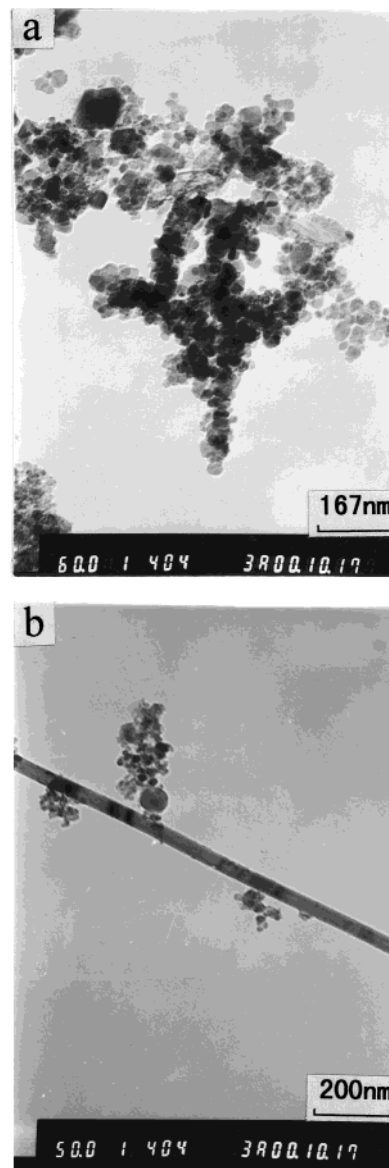
(22) Zheng, H. G.; Zeng, J. H.; Liang, J. H. *Acta Metall. Sin. (Chin. Ed.)* **1999**, *35*, 8.



**Figure 3.** TEM images of the products (a) nanocrystals $FeTe_2$ and (b) nanorods $FeTe_2$.

When hydrate hydrazine was substituted with ammonia, ethylenediamine, or pyridine, the products were iron oxides and unreacted elemental chalcogen powders rather than the desired metal chalcogenides, which was confirmed by XRD patterns. As for reaction 2, elemental chalcogens do not react directly in the alkaline medium via a simple reduction process.[23] Therefore, in the presence of a reductive atmosphere (hydrazine hydrate) and a precipitant ($Fe^{2+}$), the combination of $Fe^{2+}$ and chalcogen anions for reaction 3 can induce the chemical equilibrium (eq 2) to shift toward the right and make reactions 4 and 5 thoroughly complete. In the meantime, the $N_2$ produced continuously in the reaction autocreates an inert atmosphere as a protection,[24] and no impurities such as oxides and hydroxides were obtained, which was also proved by the XRD analysis.

The morphologies of the crystals are influenced by temperature, pressure, pH value, etc. A temperature of

(23) Wang, C.; Zhang, W. X.; Qian, X. F.; Xie, Y.; Qian, Y. T. *Mater. Chem. Phys.* **1999**, *60*, 99.
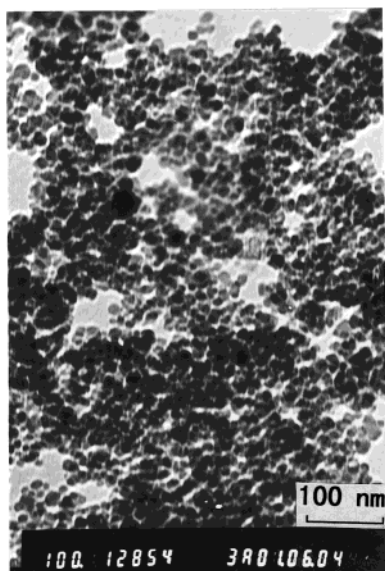(24) Chen, D. H.; Wu, S. H. *Chem. Mater.* **2000**, *12*, 1354.

**Figure 4.** TEM image of the polycrystallites $FeTe_2$ obtained at a concentration of 4.5 mmol of $FeCl_3$ in 37.5 mL of solution.

140−180 °C is probably beneficial for hexagonal $Fe_7S_8$ to grow along the plane perpendicular to the *c* axis, while the growing speed along the *c* axis is faster than that along the other two axes in the growth of $FeTe_2$. However, the oriented growth of iron chalcogenide crystals is not obvious at lower temperature (<120 °C). The $N_2$ produced apparently increases the pressure of the system, which is affirmed to have a great influence on the morphology of the produts under hydrothermal conditions.[25,26] The pressure is likely to fall into the growth stability range of the flakelike and rodlike shapes. The initial pH of the solution ($N_2H_4 \cdot H_2O$, 85% v/v) is 11. When the initial pH value is adjusted to 11−14 with 1 M NaOH, the obtained products are flakelike crystals $Fe_7S_8$ and the rodlike crystals $FeSe_2$ and $FeTe_2$. With the proceeding of the reaction, hydrazine hydrate continuously takes part in the reaction so that the basicity also decreases correspondingly. The change of the pH value possibly matches the nucleation and growth of the crystals, which is propitious for the growth of the flakelike and rodlike crystals.[27]

In the growth process of the single crystals $FeTe_2$, a suitable speed of decreasing the temperature and proper supersaturation are two important factors. The compared experiments were done at 140 °C for 12, 24, and 36 h. If the system was quickly decreased to room temperature, according to the XRD analyses, the products were all orthorhombic-phase $FeTe_2$ nanocrystals. The TEM images (Figure 3a,b) show that the products are spherelike and rodlike nanocrystals, and bulk single crystals were not obtained. Therefore, a suitable speed of decreasing the temperature (here about 0.125 °C/min) is necessary to the growth of bulk single crystals. If the quantities of $FeCl_3$ and elemental chalcogen powders were adjusted to 1.0, 3.0, 4.5, and 6.0 mmol in about 37.5 mL of solution, all of the products were orthorhombic $FeTe_2$. The single crystals were only obtained
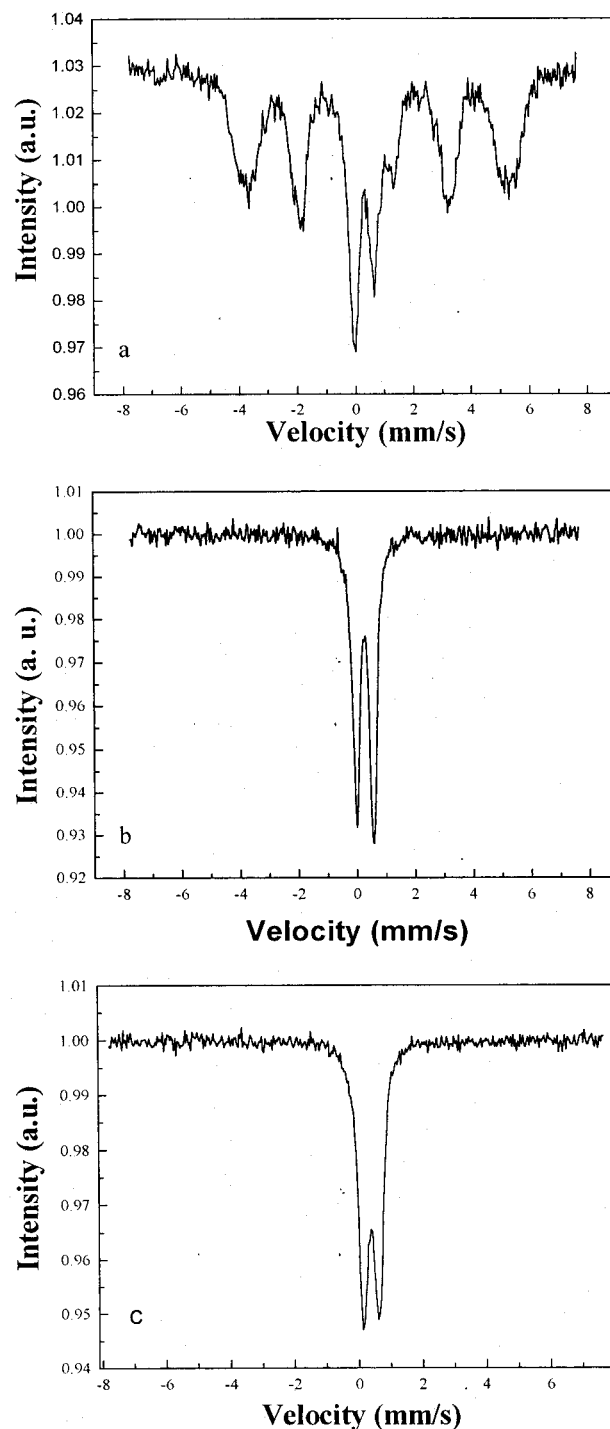
(25) Kenney, G. C. *Am. J. Sci.* **1958**, *256*, 590.
(26) Cai, Y. J.; Zhou, M. *Sci. Chin. (B)* **1993**, *23* (9), 972.
(27) Hu, J. Q.; Deng, B.; Lu, Q. Y.; Tang, K. B.; Jiang, R. G.; Qian, Y. T.; Zhou, G. E.; Cheng. H. *Chem. Commun.* **2000**, 715.

**Figure 5.** Mössbauer spectra for the samples at room temperature: (a) $Fe_7S_8$, (b) $FeSe_2$, (c) $FeTe_2$.

from the reactant concentrations of 1 and 3 mmol in 37.5 mL of solution. The higher concentration brings the solution to labile supersaturation so that the solution separates the solid powders out quickly. Meanwhile the polycrystallites $FeTe_2$ form rather than the rodlike crystals. Figure 4 shows the TEM images of the polycrystallites $FeTe_2$ obtained in the higher concentration (4.5 mmol of $FeCl_3$ in 37.5 mL of solution). A suitable speed of decreasing the temperature and proper supersaturation can make the velocity of the nucleation and growth match well and keep the solution under the metastable supersaturation conditions at all times,

**Table 2. Mössbauer Parameters of the Products at Room Temperature**

| sample | HF (kOe) | IS (mm/s) | QS (mm/s) | FWHM (mm/s) |
|---|---|---|---|---|
| $Fe_7S_8$ | 0 | 0.3179 | 0.6822 | 0.1943 |
|  | 279.88 | 0.7252 | 0.1281 | 0.3736 |
| $FeSe_2$ | 0 | 0.2832 | 0.5852 | 0.1408 |
| $FeTe_2$ | 0 | 0.3815 | 0.4774 | 0.1746 |

which ensures the perfect growth of the single crystals $FeTe_2$.

The Mössbauer spectra of the products are illustrated in Figure 5. The spectrum of $Fe_7S_8$ (Figure 5a) is fitted with a broad sextet, and the Mössbauer parameters, the isomer shift (IS), quadrupole splitting (QS), hyperfine field (HF), and full width at half-maximum (FWHM), are listed in Table 2. The hyperfine parameters of the sextet are almost in good agreement with reference values.[28] This can be interpreted as due to the presence of high-spin $Fe^{2+}$ on the octahedron lattice sites of hexagonal pyrrhotite. The vacancies in the vacancy layers in the Fe−S system have been widely studied.[9,29] The broadening of the line width could be related to the disturbance of the short-range order around Fe sites due to the random distribution of vacancies and the arrangement of S. The random distribution of vacancies in turn produces poorly resolved Mössbauer spectra as already observed elsewhere.[28,30] However, there is an apparently nonmagnetic doublet peak with IS = 0.3179 mm/s in addition to the magnetic spectra, whose peak area is around 22.6%. Kondoro[28] reported that the nonmagnetic doublets except for the outer sextets about the Mössbauer spectra of monoclinic pyrrhotite were likely to be superaramagnetic. The two-line pattern of the Mössbauer spectra for $FeSe_2$ and $FeTe_2$ (Figure 5b,c) corresponds to a typical marcasite sample. Both the doublets are asymmetric, which is attributed to a competing process between the anisotropy in the recoil-free fraction and the relaxation phenomenon as explained by Reddy and Chetty.[31] The hyperfine parameters are shown in Table 2, consistent with those reported by Fontana,[14] but different from other reported values.[32,33] This mainly results from the synthetic route, crystallization, particle size, thermal history, composition, etc. From the parameters in Table 2, it can be concluded that Fe behaves as the state similar to those of $FeTe_2$ in hybridized bonds.[14,31] Moreover, $FeSe_2$ and $FeTe_2$ exhibit nonmagnetic properties. This is because they appear antimagnetic at $T_N$ (Néel temperature, for $FeTe_2$, $T_N = 83$ K). The magnetic susceptibility will decrease when the temperature increases or decreases from $T_N$, and the antimagnetic substance becomes paramagnetic under higher temperature.[34]

## Conclusion

Low-dimensional platelike $Fe_7S_8$, rodlike $FeSe_2$ microcrystals, and $FeTe_2$ bulk single crystals have been successfully synthesized using a relatively mild HRR at 140 °C and characterized by various techniques. In this process, hydrazine hydrate plays an important role, whose basicity and reductive ability ensure the reaction process takes place. Hydrazine hydrate can coreduce $Fe^{3+}$ and elemental chalcogen to $Fe^{2+}$ and chalcogen anions, and their combination induces the reaction to be thoroughly completed. The temperature, pressure, and pH values have great influence on the morphologies of the products. As for the growth of single crystals $FeTe_2$, a suitable speed of decreasing the temperature and proper supersaturation of the solution are two important factors, which can keep the solution under the metastable supersaturation conditions. Mössbauer spectra show a magnetic property for $Fe_7S_8$ and nonmagnetic properties for $FeSe_2$ and $FeTe_2$. This method can be easily controlled and is expected to be applicable for the preparation of other chalcogenide single crystals. However, growth of inorganic bulk single crystals by this technique needs further study.

(28) Knodoro, J. W. A. *J. Alloys Compd.* **1999**, *289*, 36.
(29) Li, F.; Franzen, H. F. *J. Solid State Chem.* **1996**, *124,* 264.
(30) Kruse, O. *Am. Mineral.* **1990,** *75*, 755.
(31) Reddy, K. V.; Chetty, S. C. *Phys. Status Solidi A* **1976**, *37*, 687.
(32) Arnold, R. G. *Econ. Geol.* **1962**, *57*, 72.
(33) Temperley, A. A.; Lefevre, H. W. *J. Phys. Chem. Solids* **1966**, *27*, 85.
(34) Finlayson, D. M.; Llewellyn, J. P.; Smith, T. *Proc. Phys. Soc. London* **1959**, *74*, 75. Chiba, S. *J. Phys. Soc. Jpn.* **1955**, *10*, 837.